Osmotic dehydration of apple: Influence of sugar and water activity on tissue structure, rheological properties and water mobility

Andrea B. Nieto [a,b,1], Sebastián Vicente [e,f,1], Karina Hodara [c], María A. Castro [d], Stella M. Alzamora [a,*]

[a] Departamento de Industrias, Facultad de Ciencias Exactas y Naturales, Universidad de Buenos Aires, Ciudad Universitaria, 1428 Ciudad Autónoma de Buenos Aires, Argentina
[b] Member of Consejo Nacional de Investigaciones Científicas y Técnicas, Av. Rivadavia 1917, C1033AAJ Ciudad Autónoma de Buenos Aires, Argentina
[c] Departamento de Métodos Cuantitativos y Sistemas de Información, Facultad de Agronomía, Universidad de Buenos Aires, Av. San Martín 4453, C1417DSE Ciudad Autónoma de Buenos Aires, Argentina
[d] Departamento de Biodiversidad y Biología Experimental, Facultad de Ciencias Exactas y Naturales, Universidad de Buenos Aires, Ciudad Universitaria, 1428 Ciudad Autónoma de Buenos Aires, Argentina
[e] Professional of Comisión de Investigaciones Científicas de la Provincia de Buenos Aires, Calle 526 entre 10 y 11, 1900 La Plata, Argentina
[f] Fundación ICTB de la Cruz, Dorronzoro 141, B6700FTA Luján, Argentina

ABSTRACT

Osmotic dehydration of apple tissue (*Malus pumila*, Granny Smith cultivar) to water activity (a_w) 0.97 or 0.94 with maltose or maltose syrup solutions was studied and compared with previous results using glucose or trehalose as humectants. Structure (optical and transmission electronic microscopy observations), rheological properties (small scale dynamic oscillatory and creep/recovery measurements and large scale compression force-deformation testing), and water mobility (^{1}H NMR spectra) of parenchymatous apple tissue were significantly affected by osmotic treatments. Osmotically dehydrated apples became soft and extensible and lost crispness and hardness, while the behavior of the moduli G' and G'' indicated weaker gels after osmosis. Compression properties of the tissues abruptly changed after osmotic dehydration to a_w 0.97, while reduction to a_w 0.94 led to a compression response more similar to that of untreated apples. Compression behavior and state and distribution of water in apple tissues were influenced by the osmotic agent employed and the a_w level, while in general mechanical spectra and creep analysis were not able for distinguishing physical differences between osmotic treatments assayed.

© 2013 Elsevier Ltd. All rights reserved.

1. Introduction

At macromolecular level, physical properties of vegetables and fruits are affected, among others, by interactions between water molecules and other components. Water, besides its role as a solvent, can structure macromolecules by internal bonding and hydrophilic and hydrophobic interactions, and can act as a plasticizer making possible movement of one structure in respect to others (Lewicki, 2004). At tissue level, physical properties of produces depend on the different levels of structure and their interactions. In particular, rheological characteristics of plant tissues mainly relate to initial cell turgor, strength of cell walls and cell–cell adhesion through the middle lamella, the plasmodesms and some components located at the edges of cell faces (Alzamora et al., 2000; Waldron et al., 1997). The cell wall is an elaborated extracellular matrix enclosing each cell in a plant (Wilson et al., 2000). Models of the primary cell wall of higher plants propose that cell wall comprises three co-extensive, interpenetrating networks (Carpita and Gibeaut, 1993). A network of cellulose/hemicelluloses is embedded in a matrix of highly complex and heterogeneous pectic polymers, with structural proteins potentially forming a third domain. Extensive interactions between these independent networks are envisaged. The largest volume of the cell wall space is occupied by water, which modifies the interaction between components influencing rheological properties. Pectin-rich cell wall interfaces play a role in cell–cell adhesion while the cellulose–hemicellulose network is thought to largely contribute to rigidity (Jackman and Stanley, 1995a).

Water is a vital component in structure preservation and functional integrity of vegetable tissues. When water is removed from tissues by osmotic dehydration, water interactions with remaining constituents become more important and fruit properties are influenced by interactions water–water, water–solute, water–macromolecule and solute–macromolecule. As a consequence, great physicochemical changes in the biopolymer composition and spatial conformation occur, inducing disarrangements and/or

* Corresponding author. Tel./fax: +54 11 45763495.
E-mail addresses: andrea.bnieto@gmail.com (A.B. Nieto), sebas.vicente@gmail.com (S. Vicente), mac@bg.fcen.uba.ar (M.A. Castro), smalzamora@gmail.com, alzamora@di.fcen.uba.ar (S.M. Alzamora).
[1] These authors share the first place.

destruction of the natural structure, shrinkage, changes in water and biopolymer mobility and water distribution, color alteration and modification in mechanical properties, among others. These characteristics have been identified as the most important properties associated to modifications in quality properties of fruits. On the other hand, water loss is accompanied by solute exchange and osmotic dehydration with hypertonic sugar solutions involves the simultaneous countercurrent flow of water and sugars. The sugar selected as osmotic agent and its concentration influences the sugar uptake by the tissue. Biopolymers such as proteins and polysaccharides can change the spatial conformation under the influence of sugars (Lewicki, 2004).

Osmotic dehydration is being used in the elaboration of intermediate- and high moisture fruits, or to impregnate fruit tissues with sugars to improve the overall quality after further processing. Water activity depression in high moisture fruits is usually performed by osmotic dehydration in concentrated sugar (mono-, di- and polysaccharides) aqueous solutions, achieving after equilibration final values of a_w = 0.94–0.97 (Alzamora et al., 1995). The influence of different solutes on the kinetics and extent of water loss and solute gain has been intensively studied; however, the effect that different osmotic agents cause on fruit structure and physical properties is still unclear (Ferrando and Spiess, 2001). Understanding the impact of osmotic dehydration and type of solute on fruit physical properties is essential to design high quality osmodehydrated fruits. This paper investigated the changes in the micro and ultrastructure (by optical and transmission electronic microscopy), the rheological properties (by uniaxial compression, dynamic oscillatory shear, and creep/recovery tests) and the state of water (by ^{1}H NMR spectra determination) of apple tissues subjected to osmotic dehydration to reach a_w 0.97 or 0.94, using maltose or maltose syrup as humectants. How differences in tissue structure related to viscoelastic, compression and water mobility parameters was also explored.

2. Material and methods

2.1. Sample preparation

Fresh apples (*Malus pumila*, Granny Smith cv.) were obtained at a similar ripening stage from a local market and stored at 5 °C. Some hours prior to use, apples were removed from refrigeration and left to equilibrate at room temperature. Each fruit was hand peeled and its core was removed. Fruits were then cut into different sizes according to the analysis to be performed. Cylinders of parenchyma tissue of 15 mm in diameter and ⩾15 mm in length for compression and ^{1}H-RMN analysis and discs of 30 mm in diameter and ⩾6 mm in thickness for viscoelastic characteristics analysis were obtained using a cork borer and a razor blade. Osmotic treatments with a_w = 0.97 and a_w = 0.94 sugar aqueous solutions were carried out with apples from different batches. Untreated apple samples (without osmotic treatments) were used in each case as controls (called control 0.94 G–T and control 0.97 G–T for experiments using glucose or trehalose at a_w 0.94 and 0.97 respectively, and control M-MS for experiments using maltose or maltose syrup at both a_w values, 0.94 or 0.97).

2.2. Osmotic dehydration

Osmotic dehydration (OD) was performed at atmospheric pressure at 20 °C by immersing apple samples into a 37.3% w/w or 51.0% w/w maltose (maltose monohydrate, analytic grade Anedra S.A, Argentina) or 42.0% w/w or 56.0% w/w maltose syrup (5% w/w glucose, 48% w/w maltose, 28% w/w maltotriose and 28% w/w high sugars, food grade, Productos de Maíz S.A., Argentina)

aqueous solutions with forced convection to reach an equilibrium a_w value equal to 0.97 or 0.94 respectively. Potassium sorbate (0.15% w/w, food grade, Química Oeste S.A., Argentina) and ascorbic acid (1% w/w, food grade, Química Oeste S.A., Argentina) were added to the solutions and the pH was adjusted to 3.5 (natural pH of the fruit) with citric acid (0.5% w/w, food grade, Química Oeste S.A., Argentina) to inhibit and/or retard microbial growth and enzymatic browning (Pizzocaro et al., 1993). The stirring level was adjusted in order to turn the surface mass transfer resistance negligible. A fruit-to-solution ratio 1:20 w/w was used to minimize the dilution effect on the osmotic solutions.

The results of this research were compared with those previously obtained with apples osmotically dehydrated in a similar way but using glucose or trehalose as solutes (Vicente et al., 2012). In these experiments, apple samples were immersed into 22.0% w/w or 38.7% w/w glucose and 34.4% w/w or 48.0% w/w trehalose aqueous solutions to reach a_w 0.97 or 0.94 respectively.

Sugar concentrations to obtain a_w 0.97 or 0.94 were calculated using the equation originally proposed by Norrish (1966) with a correlation constant equal to 2.25 for glucose, 4.54 for maltose and 6.47 for trehalose (Galmarini et al., 2008), while maltose syrup concentration was determined from experimental data reported by Ceroli (2009).

At the end of OD processes (6–7 h for apple discs and 18–21 h for apple cylinders), samples were taken out of the sugar solutions, rinsed in distilled water, gently dried with tissue paper, examined for rheological and water mobility characteristics, and observed by light microscopy (LM) and transmission electron microscopy (TEM).

2.3. Measurement of compression properties

Mechanical behavior at large deformations was determined by uniaxial compression test with an Instron Testing Machine model 1101 (Canton, Massachusetts, USA) with a flat-end cylindrical probe of 35 mm diameter (10 mm/min cross-head speed, 500 N load range, 80% deformation, 25 °C). From force-deformation curves (30 replicates for each condition), true stress (σ_R) (Eq. (1)) and Hencky strain (ε_R) (Eq. (2)) were calculated assuming constant sample volume during compression. Deformability modulus (E_d) was obtained from the slope of the initial linear zone of the stress–strain curve (Eq. (3)). True rupture stress (σ_R^R) and strain at $\sigma_R^R(\varepsilon_R^R)$ were determined from the first peak of the stress–strain curve as described by Peleg (1984). Toughness (W) (i.e. the energy absorbed by the material up to the rupture point per unit of volume of the apple cylinder) was obtained by calculating the area of the stress–strain curve until the rupture point (Eq. (4)) (Calzada and Peleg, 1978).

$$\sigma_R = F(t) \cdot [H_0 - H(t)]/A_0 \cdot H_0 \tag{1}$$

$$\varepsilon_R = ln[H_0/H_0 - \Delta H] \tag{2}$$

$$E_d = \sigma_R/\varepsilon_R \tag{3}$$

$$W = \int_{s_0}^{s_R} \sigma \partial\varepsilon \tag{4}$$

where $F(t)$ is strength at time t, H_0 is the initial height sample, ΔH is the absolute reduction of the original height in the direction of the applied force, A_0 is the initial specimen area, $H(t)$ and H_0 are the height of the cylinder at the time of compression t and $t = 0$ respectively.

2.4. Measurement of viscoelastic properties

Mechanical spectra and creep/recovery curves were determined at 20 °C in a Paar Physica MCR 300 controlled strain rheometer (Anton Paar GmbH, Graz, Austria) using a 30 mm diameter parallel

plate head geometry with rough surface (model PP/30) and 1N of compression to provide maximum contact area and minimum slip. Temperature was controlled by an external liquid bath thermostat model Viscotherm VT2 (Anton Paar GmbH, Graz, Austria). For both tests, data were obtained using a minimum of 11 replicates.

Dynamic oscillatory tests were performed in the controlled strain mode. To determine the linear viscoelastic range (LVR), prior to the frequency sweep, an amplitude strain sweep was carried out at an angular frequency of $10 \, s^{-1}$. The limits of linearity were established using the US 200 software package (Paar Physica, Graz, Austria). Storage (G') and loss (G'') modules were then measured in the frequency range 0.1–$100 \, s^{-1}$ using a strain amplitude value of 0.05%, within the limits of the previously established linearity. The storage modules spectra data were fitted using a linear regression:

$$\log(G') = m \log(\omega) + k \tag{5}$$

where m is the slope and k is the $\log(G')$ at $1 \, s^{-1}$ of angular frequency (ω).

Creep-recovery tests were conducted by applying a constant shear stress of 35 Pa for 100 s. After removal of the stress, sample recovery was registered for an additional period of 200 s. A previous stress sweep indicated that in the selected conditions deformation was proportional to the stress. Previously to the creep assay, the sample was subjected to two repeat loading (60 s) and unloading (120 s) cycles to remove any surface irregularity in the specimen (Mittal and Mohsenin, 1987).

Compliance response was fitted with a mechanical model consisting of a spring in series with two Kelvin–Voigt elements and a dashpot element (Sherman, 1970; Jackman and Stanley, 1995b) described by the following equation:

$$J(t, \tau) = (J_0) + \sum_{i=1}^{2} (J_i)\left(1 - e^{-t/\lambda_i}\right) + (t/\eta_0) \tag{6}$$

where $J(t, \tau)$ is the creep compliance ($= \gamma(t)/\tau$ with $\gamma(t)$ being the strain at the time t and τ the constant stress applied); J_0 is the instantaneous compliance at $t = 0$; J_i are the retarded compliances; λ_i ($= \eta_i \times J_i$) are the retardation times and η_i are the coefficients of viscosity associated with the Kelvin–Voigt elements; η_0 is the coefficient of viscosity associated with Newtonian flow and its inverse the steady-state fluidity of the material. J_0 would be related to those bonds of structural units that are elastically stretched when the stress is applied, and show instantaneous and complete recovery when the stress is removed. J_i parameters would be related to bonds that break and reform at different rates, the weaker bonds breaking at smaller values of time than the stronger ones. They show retarded elastic recovery. The linear region of Newtonian compliance t/η_N would be related to those bonds that are ruptured during the shear creep step and the time required for them to reform is longer than the creep-recovery period; the released units will flow and part of the structure is not recovered (Sherman, 1970).

Linear and nonlinear regression procedures were made using the Origin v6 (Microcal Sofware Inc., USA) software with Levenberg–Marquardt iteration method to fit the nonlinear curves.

2.5. Determination of moisture, soluble solid contents and a_w

The weight fraction of water per cent (x_w, wet basis) in apples was determined gravimetrically using a vacuum oven (Gallenkamp, United Kingdom) at 65 °C over calcium chloride as desiccant until constant weight.

Soluble solid content percentage (z_{ss}, wet basis) in the sample liquid phase was analyzed by measuring the refraction index in two refractometers (Atago, model PR 101 and model PR 200, Japan) at 25 °C.

The a_w was measured with a psycrometer (Aqua-Lab CX-2, Decagon Devices Inc., Pullman, USA.) at 20 °C and calibrated with saturated aqueous solutions (Resnik et al., 1984).

Determinations were made in triplicate and the average was reported.

2.6. Microscopic studies

For LM of fresh and osmotically dehydrated samples, cubes of approximately $3 \, mm^3$ taken from the central zone of the apple sample were fixed twice in 3% w/w glutaraldehyde solution and then in 0.1 M potassium phosphate buffer (pH 7.4) overnight at room temperature. Cubes were then rinsed three times with distilled water, postfixed in 1.5% w/w OsO_4 solution at room temperature and dehydrated in a graded acetone series prior to being embedded in low viscosity Spurr resin (Sorrivas and Morales, 1983). Sections (1–2 μm thick) of the Spurr-embedded tissue were cut on a Sorvall MT2-B ultracut microtome and stained with aqueous 1% w/w toluidine blue and 1% w/w basic fuchsin solutions and examined in a Axiscope 2 Plus light microscope (Carl Zeiss, Jena, Germany). For TEM, ultrathin sections were collected on copper grids, double stained with uranyl acetate and lead citrate (Reynolds, 1963) and examined using a JEOL JEM 1200 EX II transmission electron microscope at an accelerating voltage of 80 kV.

All reagents were from Merck Química Argentina S.A. (Argentina).

2.7. Water mobility analysis

Transverse relaxation times (T_2) were determined at 40.0 °C in a low-resolution ^{1}H pulsed nuclear magnetic resonance spectrometer ^{1}H NMR Minispec PC/120 series NMR analyzer (Bruker, Karlsruhe, Germany) with an operating pulse of radio frequency radiation of 20 MHz, using the Carr–Purcell–Meiboom–Gill (CPMG) sequence with a τ value (time between 90° and 180° pulse) of 2 ms. The data were acquired as 8 scan repetitions, with a recycle delay of 4 s between each scan.

NMR relaxation signals were expressed mathematically as the sum of exponential decays according to the following equation:

$$Y = (y_0) + \sum_{i=1}^{n} (A_i)(e^{-t/T2i}) \tag{7}$$

where Y represents the NMR signal intensity at time t and n the number of uni-exponentials. The time constant associated with uni-exponential decay or relaxation time T_{2i} corresponds to the mobility of protons in the water fraction i, and A_i reflects the apparent water content and is proportional to the number of protons in the T_{2i} state. From A_i values, normalized C_i values were obtained according to the expression:

$$C_i = A_i/(A_1 + A_2 + \cdots + A_n) \cdot 100 \quad \text{with } i = 1, 2, \ldots, n \tag{8}$$

Data were averaged over 6 replicates for each treatment. The Origin v6 (Microcal Sofware Inc., USA) software with Levenberg–Marquardt iteration method was used to fit the nonlinear curves. The residuals were used together with the correlation coefficient to estimate the correct number of exponential decays.

2.8. Statistical analysis

Osmotic treatments were made using a different batch of apples for each a_w assayed and the statistical analysis was carried out considering both controls.

Data were analyzed using multivariate analysis of variance (MANOVA) (Quinn and Keough, 2002). Post-hoc multiple comparisons among multivariate means of treatments were performed by

Hotelling tests based on Bonferroni correction. Discriminant function analysis (DFA) was applied as an extension of multivariate analysis of variance (McGarigal et al., 2000). Before conducting the analyses, the assumptions of homogeneity of variance–covariance matrices and multivariate normal distribution were tested. Multivariate outliers were detected by Mahalanobis distance and removed from the data set. Multicolinearity among response variables was assessed by the Pearson correlation matrix, and only uncorrelated variables were entered into the MANOVA and DFA analyses. Logarithmic transformation of data was necessary in some cases for proper use of the statistical procedure. Values of $p < 0.05$ were considered to be significant in all analyses.

Statistical analyses were carried out using InfoStat Versión 2011 (InfoStat Group, FCA – Universidad Nacional de Córdoba, Argentina).

3. Results and discussion

3.1. Moisture, soluble solid contents and a_w changes

Osmotic treatment decreased water content and increased soluble solids content in apple tissues (Table 1). For a given solute, apple samples immersed in solutions with a_w 0.94 exhibited the greatest loss of water and solute gain due to the large difference in the chemical potentials of water and solute between osmotic solutions and the fruit. For a given a_w, there was less moisture loss and soluble solids gain when the monosaccharide glucose was used.

3.2. Micro and ultrastructure changes

Changes in microstructure and ultrastructure of apple tissues induced by osmotic treatments were examined by LM and TEM observations (Figs. 1 and 2). Cytological examination of untreated or fresh apple revealed turgid cells with intact plasmalemma and tonoplast, plasma membrane intimately associated with the wall and parietal cytoplasm (Figs. 1A and 2A). Tissues showed intercellular spaces of different sizes and shapes (Fig. 1A). Cell walls appeared with tightly packed and darkly stained fibrillar material, organized in a longitudinal or a loose reticulate pattern according to the region (Fig. 2 A). The middle lamella cementing adjacent cells was much stained (Fig. 2A).

Osmotic dehydration to a_w 0.97 induced a loss of turgor pressure, since the cytoplasm retracted from the cell wall and/or cell membranes appeared broken (Fig. 1B–I). After osmotic dehydration in 22% w/w glucose solution, apple tissue exhibited cells clearly affected by plasmolysis (Fig. 1B). In many cells membranes kept their integrity but looked collapsed, with a severe reduction of their surfaces and formation of vesicles. Walls appeared slightly

less smoothed but not collapsed. Cells were more or less regular in shape, with an arrangement similar to that of fresh fruit. In TEM, cell walls in general appeared with good electron density and a notorious middle lamella (Fig. 2B). Apple tissues treated with 34.4%w/w trehalose solution 37.3% w/w maltose solution and 42.0% w/w maltose syrup solution showed a slight shrinkage, reflecting their lower equilibrium moisture content compared with glucose treated ones at the same a_w (Fig. 1C–E). Trehalose and maltose had a more protective effect on membranes than glucose: membrane integrity had been maintained in most of the cells; overall plasmalemma and tonoplast had not collapse. Shrunk protoplasts appeared with an unusual round shape in the centre of many trehalose treated cells (Fig. 1C) while maltose treated cells exhibited not broken but slightly more collapsed membranes (Fig. 1D). Rupture of the plasma membrane and tonoplast was noticeable in cells osmotically dehydrated with maltose syrup, which also showed a notorious decrease in cell-to-cell contact (Fig. 1E). In TEM, walls of trehalose treated cells exhibited dark staining, with a clear middle lamella cementing neighboring cell walls and a tightly fibrillar packing irregularly stained (Fig. 2C). In maltose dehydrated cells, walls were detected with a uniform staining and the middle lamella appeared thicker than in the raw fruit. Walls in maltose syrup treated cells were less smooth, very undulated and with good electronic density, but the middle lamella was not visualized in many places (Fig. 2E). Plasmodesmata looked well preserved in glucose, trehalose and maltose treated fruits (TEM micrographs not shown) and can be clearly noticed as dark punctuations in the apple walls visualized in Fig. 1B–D.

The reduction to 0.94 in a_w of the osmotic solutions affected apple structure at cellular level in a more severe way than at a_w 0.97 (Figs. 1 and 2F–I). As a result of increased dehydration, apple tissues dehydrated-impregnated with 38.7% w/w glucose solution, 48.0% w/w trehalose solution, 51.0% w/w maltose solution and maltose syrup solution displayed a more important cytoplasm contraction/rupture of membranes than at a_w 0.97. In general, membranes disruption was generalized in glucose, maltose and maltose syrup treated tissues (Fig. 1F, H, and I) while collapse of protoplast and membranes (although many of them without rupture) was detected in trehalose containing tissues (Fig. 1G). Cell walls appeared stained but much deformed and folded, with a very sinuous contour, mainly in glucose and maltose syrup treated apples (Fig. 1F and I). In images acquired with TEM, the middle lamella of glucose or maltose syrup treated walls was rarely visualized (Fig. 2F and I). On the contrary, the middle lamella of trehalose and maltose treated tissues appeared clearly reinforced, very well defined and thick, with a longitudinal pattern staining in trehalose containing tissue and a transversal one in tissue with maltose, denoting an specific effect of these disaccharides on wall pectin molecules (Fig. 2G and H). In both tissues, cellulose fibrils appeared

Table 1
Means of weight fraction of water (x_w), soluble solids (z_{ss}) and a_w of control (fresh) and osmotically dehydrated apples.

| Treatment	$x_w \pm$ SD (%)	$z_{ss} \pm$ SD (%)	$a_w \pm$ SD
Control	86.52 ± 1.04	10.3 ± 0.5	0.98 ± 0.01
Samples immersed in:			
22.0% w/w glucose solution	76.1 ± 0.72	23.4 ± 0.1	0.97 ± 0.01
34.4% w/w trehalose solution	62.6 ± 0.48	32.9 ± 0.8	0.97 ± 0.06
37.3% w/w maltose solution	62.0 ± 0.64	34.6 ± 1.1	0.97 ± 0.01
42.0% w/w maltose syrup	62.1 ± 0.83	33.7 ± 0.8	0.97 ± 0.01
38.7% w/w glucose solution	59.9 ± 0.59	34.4 ± 1.0	0.94 ± 0.01
48.0% w/w trehalose solution	48.7 ± 2.86	44.6 ± 0.1	0.94 ± 0.01
51.0% w/w maltose solution	44.7 ± 1.90	50.5 ± 1.9	0.94 ± 0.01
56.0% w/w maltose syrup	47.0 ± 1.27	48.7 ± 1.2	0.94 ± 0.01

SD: standard deviation.
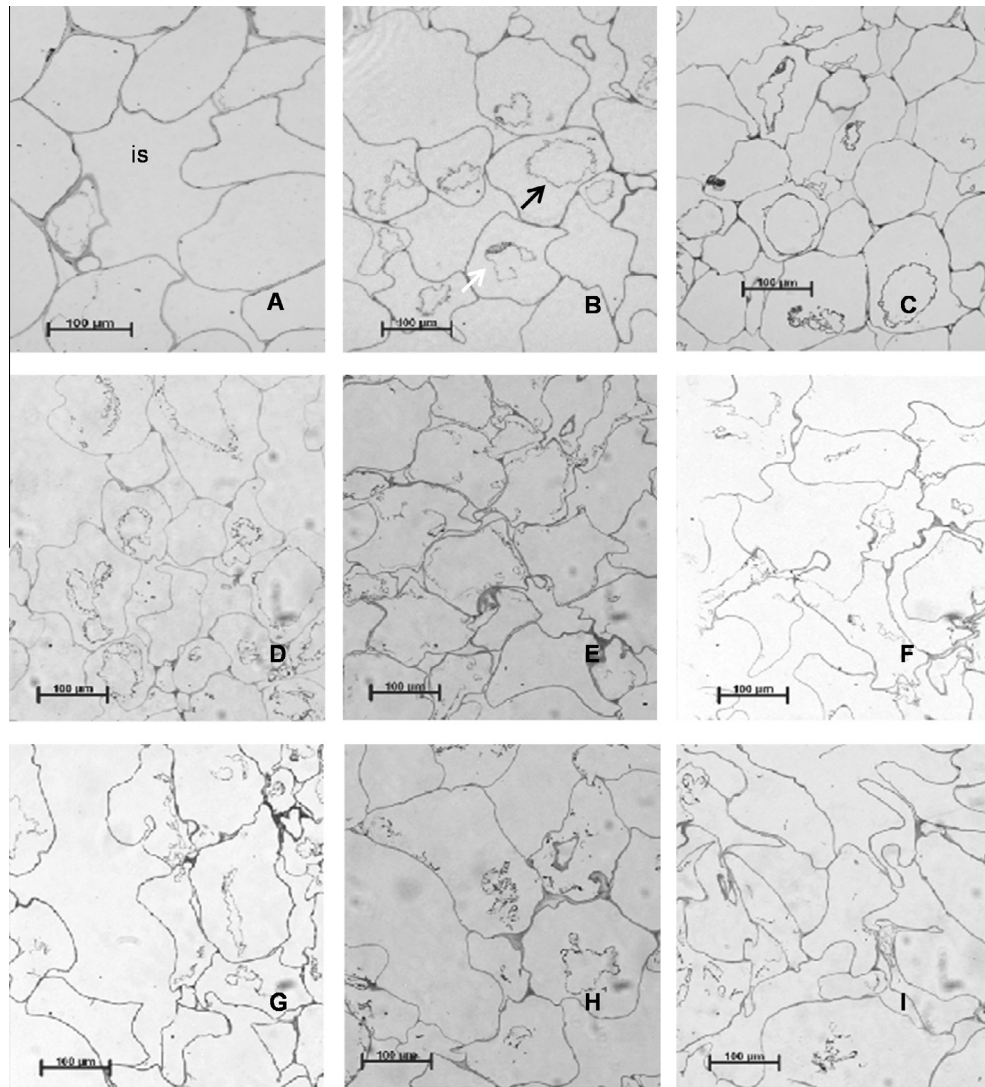
Fig. 1. LM micrographs of parenchyma apple tissue. (A): control. (B–E): osmotically dehydrated in a_w 0.97 solutions. (F–I): osmotically dehydrated in a_w 0.94 solutions. (B and F): glucose solutions. (C and G): trehalose solutions. (D and H): maltose solutions. (E and I): maltose syrup solutions. Scale: 100 μm. ie: intercellular space; black arrow: plasmolysed cytoplasm; white arrow: broken membranes.

tightly packed and electron-dense, with a clear intermixed arrangement. Tissues osmotically dehydrated in maltose syrup solution showed a slightly reduced staining of walls (Fig. 2I) and, in some images (not shown), fibrillar distribution became striated, with regions of high and low electronic density.

In spite of the type of solute, plasmodesmata appeared to maintain their structural integrity in all tissues dehydrated to a_w 0.94 (micrographs not shown), remaining a point of connection between the cells, holding them together. Also, electron-dense material located at the corner of tricellular junctions and intercellular spaces could be detected in all treated (a_w 0.97 and 0.94) and untreated tissues, evidencing the cell adhesion through the edges of the cell faces. This is worth noting in maltose syrup treated cells, where the middle lamella (other cementing element between cells) could hardly be visualized.

Disaccharides, such as trehalose and maltose, have been widely used as stabilizers during dehydration (Patist and Zoerb, 2005; Crowe et al., 1996). The ability to form glasses and direct interaction between the sugar and polar groups in proteins and phospholipids would be responsible for stabilization. As tissues are dried,

hydrogen bonding between trehalose and the polar lipids of biomembranes has been demonstrated to replace the water of hydration at the membrane–fluid interface, preventing the phase transition from lamellar to gel phase and the consequent leakage. This effect, not shown by glucose, can be clearly visualized in Fig. 1C. Trehalose and maltose are chemical isomers but stabilizing effect of maltose on plasmalemma would be lower, as shown in Fig. 1D. As reviewed by Patist and Zoerb (2005), the superior protecting properties of trehalose with respect to maltose would be due to the higher trehalose's ability to disrupt the water structure (the heat of solution values were 19.1 kJ/mol and 15.6 kJ/mol for trehalose and maltose respectively). Fig. 2H also showed that maltose participated in the network of hydrogen bonds of pectic substances, fact that was yet reported in the previous work by Vicente et al. (2012) regarding trehalose (Fig. 2G).

3.3. Rheological characterization

3.3.1. Compression response

Typical true stress *vs.* true strain curves, generated during compression of apple cylinders, are shown in Fig. 3. Compression
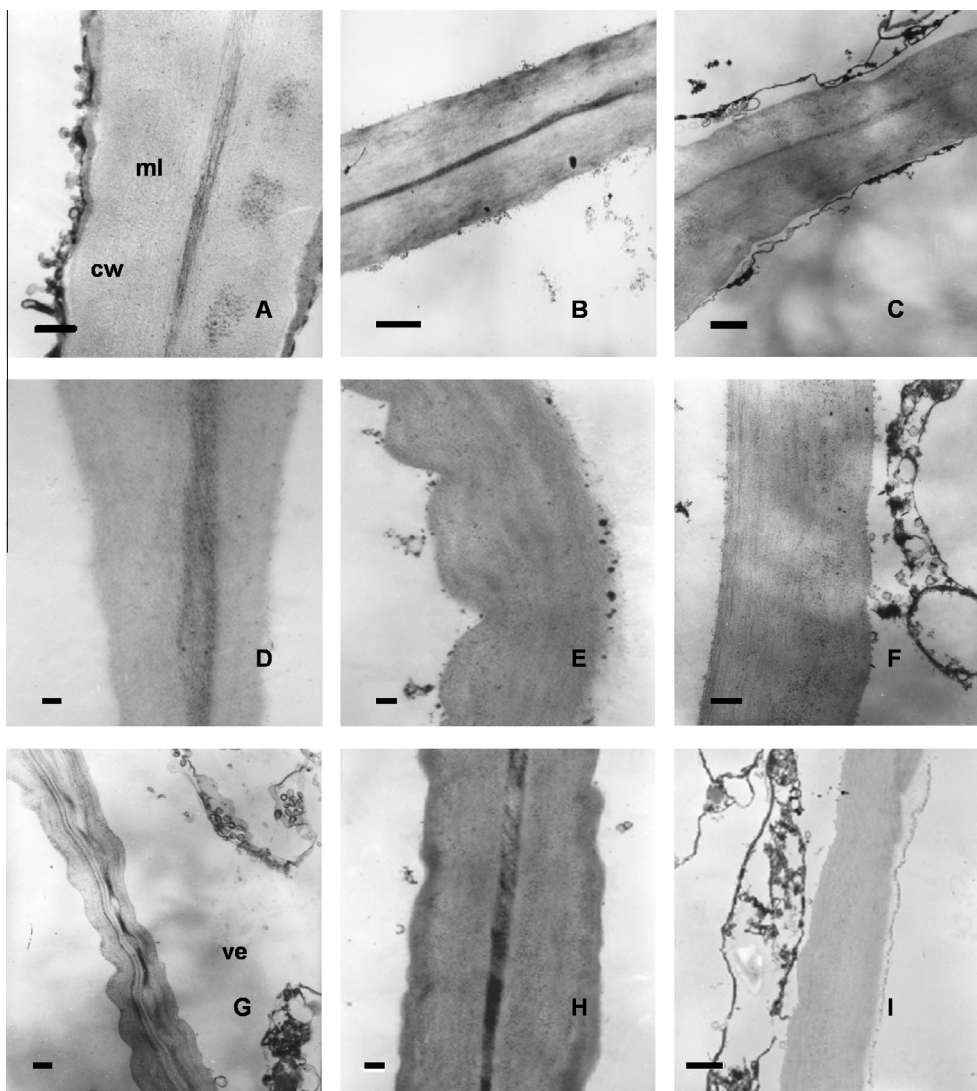
Fig. 2. TEM micrographs of parenchyma apple tissue. (A): control. (B–E): osmotically dehydrated in a_w 0.97 solutions. (F–I): osmotically dehydrated in a_w 0.94 solutions. (B and F): glucose solutions. (C and G) trehalose solutions. (D and H): maltose solutions. (E and I): maltose syrup solutions. Scale: (F–H): 500 nm; (B, C, I): 1 μm; (A, D, E): 200 nm. cw: cell wall; ml: middle lamella; ve: vesicle.

curves of fresh apple samples exhibited the typical shape of hard materials, with low resistance to deformation and abrupt rupture peaks, followed by successive fracture events characteristic of crisp tissues. Osmotic dehydration processes resulted in weaker and softer tissues, with lower rupture stress and higher resistance to deformation, although these changes depended on the type of solute and the final a_w level. In general, for a given solute, true stress increased and strain at rupture point decreased as a_w value was reduced from 0.97 to 0.94. At a_w 0.94, after a small linear part in the curve stress vs strain, the behavior of dehydrated tissues became non-linear and strain-hardening occurred, as the stress increased more rapidly with strain. Table 2 shows the mean and the standard deviations values corresponding to the mechanical parameters of examined samples (Eqs. (1)–(4)). The MANOVA of treatments was highly significant for compression measurements ($F_{30,924}$ = 59.25; P < 0.0001). The 94.5% and the 3.8% of the variance in the original variables were respectively explained by the first and the second discriminant functions derived from DFA. The most important discriminating selective variable among treatments was the deformation at the rupture point ε_R^R and, in to a lesser degree, the rupture energy W, followed by the rupture strength σ_R^R. 70%

(n = 319) of random apple samples were successfully classified by treatments from DFA. The corresponding canonical scores bi-plot for the first two discriminant functions (figure not shown) showed a clear separation between controls and osmotically dehydrated apples, which exhibited higher ε_R^R values. Compression test results statistically differentiated the type of solute at both a_w assayed as well as the a_w level for a given solute. Overall apples impregnated with trehalose at a_w 0.97 exhibited the greatest ε_R^R values, while apples impregnated with maltose and maltose syrup showed the lowest W values at both a_w levels. For a given solute, the strength and the rupture energy were higher at the lowest a_w, while the deformation at the rupture point was lower, except for maltose. Apples dehydrated with 0.97 a_w maltose solution showed the highest E_d and the lowest ε_R^R values among treated samples. At both concentrations, maltose impregnated samples also exhibited the highest σ_R^R of dehydrated samples.

Numerous structure changes may have a significant impact on compression behavior. The mechanical of osmotically dehydrated tissues can be explained in part by the loss of turgor. It is well known that fresh tissues containing turgid cells are crisper and
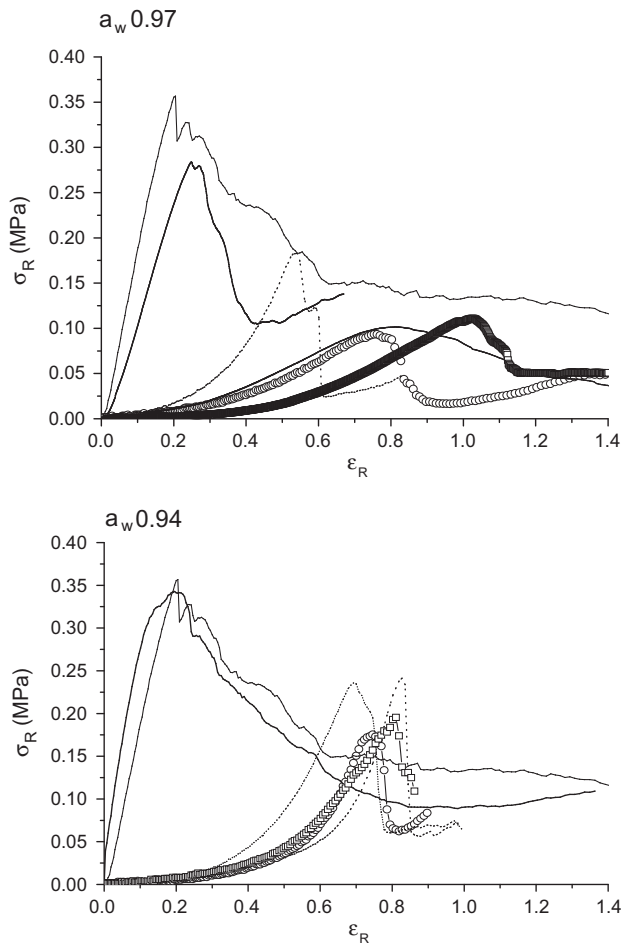
Fig. 3. Typical compression curves of true stress vs. true strain for controls and apples osmotically dehydrated in aqueous solutions of glucose or trehalose at a_w = 0.97 or a_w = 0.94. (━━━) control 0.97 G–T (for a_w 0.97) or 0.94 G–T (for a_w 0.94), (—) control M-MS, (▪▪▪) maltose, (□) trehalose, (○) maltose syrup, (·······) glucose.

work-of-fracture (Waldron et al., 2003) than non turgid ones, but W values showed in Table 1 did not show any defined trend, probably due to the complexity of phenomena involved in the mechanical response. Besides loss of turgor, softening ($< \sigma_R^R$) of treated tissues occurred as a result of a weakening of intercellular adhesion, reorientation of cellulose fibrils and folding of walls and degradation/solubilization of wall biopolymers. As expected, the reinforced of the middle lamella could be the responsible for the high σ_R^R and E_d values in maltose containing tissues; however, the high electronic dense middle lamella layer did not result in an increased firmness of apple tissues impregnated with trehalose. Cellular collapse and greater solid concentration of 0.94 a_w tissues would explained the higher σ_R^R and lower ε_R^R values compared with 0.97 a_w samples.

Tissue failure can involve cell separation or cell rupture (or a combination of both phenomena), depending on whether cell walls are stronger than the forces holding cells together or forces adhering cells to one other are stronger than the cell walls respectively (Waldron et al., 2003; Lillford, 2001). In spite of the reduction in cell-to-cell adhesion (in different degree according to the solute and the a_w level), plasmodesmata and electronic dense edge of cells observed in microscopic images could act as points of wall rupture in softened treated tissues where most of the wall have separated, ensuring cell breakage (Waldron et al., 2003). So, tissue fracture of treated apples would involve wall rupture or at least a combined mechanism.

3.3.2. Dynamic oscillatory shear response

Osmotic treatments caused a decrease in both modules, G' and G'' (mechanical spectra are not shown). However, for all samples, G' was much greater than G'' and the material behaved more like a solid, that is, the deformations would be mainly elastic or recoverable. The lost factor (tang $\delta = G''/G'$) ranged between 0.08 and 0.21 without a defined trend. Because of a value reduction in the complex modulus $G^*((G'^2 + iG''^2)^{1/2})$ in treated apples, a decrease in the total shear stiffness occurred, arising from both viscous flow and elastic strains. The mechanical spectra of fresh and osmotically dehydrated samples showed a very weak linear dependence of G' (m ranged from 0.053 to 0.061 for control and from 0.067 to 0.082 for osmotically dehydrated samples), typical of viscoelastic cross-linked network-type structures (Table 3) (Khan et al., 1997). MANOVA showed significant differences in the linear relationship log $G' - log\omega$ between untreated and treated apples. The slightly higher m values of treated apples compared with raw apple evidenced a weakening of the network structure. How-

characterized by greater stiffness ($>E_d$) and lower resistance to deformation ($< \varepsilon_R^R$) than tissues containing cells with low turgor pressure. It has also been argued that turgid tissues exhibit lower

Table 2
Compression parameters (mean values) for controls and osmotically dehydrated apples.

Treatment	σ_R^R (MPa) ± SD	ε_R^R ± SD	E_d (MPa) ±SD	W (MJ/m^3) ±SD	
Control 0.97 G–T[a]	0.33 ± 0.04	0.26 ± 0.02	1.7 ± 0.2	44 ± 8	A
Control 0.94 G–T[b]	0.34 ± 0.03	0.19 ± 0.02	2.1 ± 0.3	37 ± 7	B
Control M-MS[c]	0.35 ± 0.04	0.19 ± 0.02	2.2 ± 0.3	35 ± 5	B
Samples immersed in:					
22.0% w/w glucose solution	0.11 ± 0.02	0.79 ± 0.06	0.04 ± 0.01	37 ± 6	C
34.4% w/w trehalose solution	0.12 ± 0.02	1.02 ± 0.07	0.02 ± 0.01	36 ± 5	D
37.3% w/w maltose solution	0.17 ± 0.04	0.61 ± 0.06	0.06 ± 0.02	30 ± 8	E
42.0% w/w maltose syrup	0.10 ± 0.03	0.75 ± 0.07	0.04 ± 0.01	26 ± 6	F
38.7% w/w glucose solution	0.23 ± 0.04	0.64 ± 0.08	0.05 ± 0.02	41 ± 7	G
48.0% w/w trehalose solution	0.22 ± 0.07	0.81 ± 0.07	0.03 ± 0.01	42 ± 6	H
51.0% w/w maltose solution	0.25 ± 0.05	0.82 ± 0.09	0.02 ± 0.01	37 ± 4	I
56.0% w/w maltose syrup	0.17 ± 0.03	0.69 ± 0.09	0.04 ± 0.01	28 ± 4	J

Post-hoc multiple comparisons using Hotelling tests based on Bonferroni correction α = 0.05.
Different letters indicate significant differences at $p \leqslant 0.0001$.
SD: standard deviation; σ_R^R: true rupture stress; ε_R^R: strain at σ_R^R; E_d: deformability modulus; W: toughness.
[a] Controls for the fruit batch used for tests with glucose and trehalose at a_w 0.97.
[b] Controls for the fruit batch used for tests with glucose and trehalose at a_w 0.94.
[c] Control for the fruit batch used for tests with maltose and maltose syrup at a_w 0.97 and 0.94.

Table 3
Parameters of log G' vs log ω (Eq. (5)) for controls and osmotically dehydrated apples.

Treatment	$m \pm SD$	$k \pm SD$	Correlation coefficient	
Control 0.97 G–T[a]	0.061 ± 0.006	5.36 ± 0.08	⩾0.9	A
Control 0.94 G–T[b]	0.062 ± 0.006	5.37 ± 0.08	⩾0.9	A
Control M-MS[c]	0.053 ± 0.003	5.46 ± 0.06	⩾0.9	A
Samples immersed in				
34.4% w/w trehalose solution	0.069 ± 0.005	4.63 ± 0.07	⩾0.99	B
37.3% w/w maltose solution	0.081 ± 0.006	4.53 ± 0.04	⩾0.99	C
42.0% w/w maltose syrup	0.067 ± 0.002	4.45 ± 0.04	⩾0.99	E
38.7% w/w glucose solution	0.070 ± 0.003	4.45 ± 0.04	⩾0.99	D E
48.0% w/w trehalose solution	0.070 ± 0.005	4.52 ± 0.07	⩾0.99	B E
51.0% w/w maltose solution	0.078 ± 0.007	4.42 ± 0.08	⩾0.99	D
56.0% w/w maltose syrup	0.071 ± 0.004	4.43 ± 0.09	⩾0.99	D E
34.4% w/w trehalose solution	0.082 ± 0.003	4.64 ± 0.05	⩾0.99	C

Post-hoc multiple comparisons using Hotelling tests based on Bonferroni correction $\alpha = 0.05$.
Different letters indicate significant differences at $p \leqslant 0.0001$.
SD: standard deviation.
[a] Controls for the fruit batch used for tests with glucose and trehalose at a_w 0.97.
[b] Controls for the fruit batch used for tests with glucose and trehalose at a_w 0.94
[c] Control for the fruit batch used for tests with maltose and maltose syrup at a_w 0.97 and 0.94.

ever, overall, G' values did not allow distinguishing differences between the osmotic treatments assayed, neither regarding the type of solute nor its concentration.

The elastic behavior (and so G' response) of fruit tissues has been attributed to the cellulose (which provides walls with rigidity and resistance to rupture), the occlude air in the fruit matrix, and the turgor pressure (which together with the cell wall leads to the rigidity of the tissues and the support for maintaining cell and tissue shape) (Pitt, 1992; Alzamora et al., 2008; Carpita and Gibeaut, 1993). The main responsible for decreased G' values would be the loss of turgor, the reduction of intercellular spaces and the air–liquid exchange during osmosis.

3.3.3. Creep/recovery response

Representative creep/recovery curves for fresh and treated samples are presented in Fig. 4. Osmotic treatments caused relevant changes in both creep strain at 100 s and residual strain after an additional 200 s recovery. For the time scale of the experiments, the creep response of fresh and treated tissues was well characterized (correlation coefficient >0.999) by the mathematical model represented by Eq. (6) and the corresponding parameters are supplied in Table 4. MANOVA of treatments was highly significant for creep behavior ($F_{40,564} = 7.16$, $p < 0.0001$). Creep parameters showed significant differences between fresh and treated samples but multivariate means of apples subjected to the different osmotic treatments did not differ statistically except when treatment was performed using glucose solution with a_w 0.97. Glucose-a_w 0.97 treated apples were characterized by the lowest values of J_0, J_1, J_2 and $1/\eta_0$ among apples that underwent osmotic treatments. The other osmotic treatments caused approximately a 6–11-fold increase in the instantaneous elastic compliance J_0 relative to the untreated apple, revealing a decrease in the instantaneous elastic modulus E_0 (=$1/J_0$), while the increase in viscoelastic compliances J_1 and J_2 and in steady-state viscous compliance $1/\eta_0$ ranged from 6 to 13-fold, from 10 to 14-fold and from 5 to 14-fold respectively. DFA correctly classified the treatments of 51.3% ($n = 152$) of the random apple sample test data. This small percentage could be due to the greater error associated with creep/recovery measurements (Alzamora et al., 2008). The first discriminant function accounted for 98.34% of the variation while the second one accounted for only 1.29% of the variation, being J_0 and η_0 the most significant discriminating selective variables among treatments which contributed to the first and the second discriminant functions respectively.
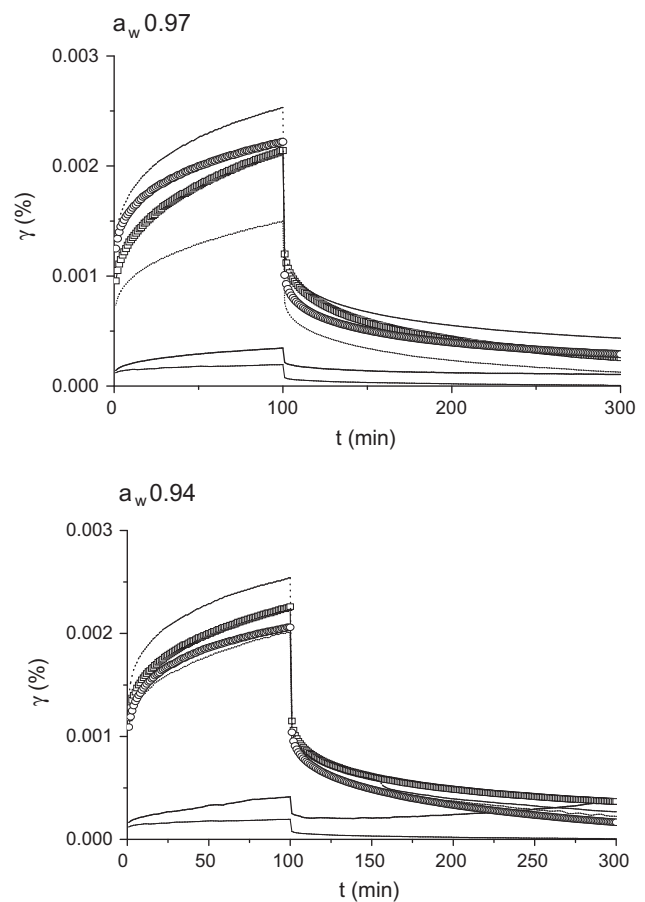

Fig. 4. Typical experimental creep/recovery curves (deformation γ vs time t) for controls and apples osmotically dehydrated in aqueous solutions of glucose or trehalose at $a_w = 0.97$ or $a_w = 0.94$. (▬▬) control 0.97 G–T, (—) control 0.94 G–T, (▪▪▪▪) maltose, (□) trehalose, (○) maltose syrup, (······) glucose.

Osmotic treatments resulted in minor changes in the contribution of each type of compliance to overall compliance (data not shown). All samples exhibited plastic strain which remained unrecovered after the creep/recovery test. Plasticity values (the ratio of unrecoverable or permanent deformation, t/η_0, to the total

Table 4
Viscoelastic parameters (mean values) derived by fitting Eq. (6) to compliance curves from creep phase for controls and osmotically dehydrated apples.

Treatment	$J_0 \times 10^6$ (1/Pa) ±SD	$J_1 \times 10^6$ (1/Pa) ±SD	$J_2 \times 10^6$ (1/Pa) ±SD	λ_1 (s) ±SD	λ_2 (s) ±SD	$\eta_0 \times 10^{-7}$ (Pa s) ±SD	Correlation coefficient	
Control 0.97 G–T[a]	4 ± 1	2.3 ± 0.3	0.9 ± 0.3	30 ± 12	3 ± 2	5 ± 2	⩾0.999	B
Control 0.94 G–T[b]	3 ± 1	2 ± 1	0.9 ± 0.3	31 ± 15	2 ± 1	9 ± 2	⩾0.999	A
Control M–MS[c]	3.2 ± 0.4	1.1 ± 0.2	0.7 ± 0.1	25 ± 9	2 ± 1	11 ± 3	⩾0.999	B
Samples immersed in:								
22.0% w/w glucose solution	21 ± 2	9 ± 2	5 ± 1	27 ± 7	2.8 ± 0.4	1.05 ± 0.06	⩾0.999	C
34.4% w/w trehalose solution	27 ± 3	18 ± 3	9 ± 3	30 ± 7	2.7 ± 0.4	0.6 ± 0.1	⩾0.999	D
37.3% w/w maltose solution	35 ± 4	15 ± 3	9 ± 2	22 ± 2	2.5 ± 0.1	0.8 ± 0.1	⩾0.999	D
42.0% w/w maltose syrup	32 ± 5	13 ± 3	8 ± 2	23 ± 4	2.5 ± 0.3	0.9 ± 0.2	⩾0.999	D
38.7% w/w glucose solution	28 ± 2	12 ± 2	7.3 ± 0.8	22 ± 2	2.2 ± 0.2	0.9 ± 0.2	⩾0.999	C,D
48.0% w/w trehalose solution	32 ± 5	15 ± 3	9 ± 2	21 ± 3	2.3 ± 0.3	0.8 ± 0.2	⩾0.999	D
51.0% w/w maltose solution	36 ± 6	15 ± 3	10 ± 2	22 ± 3	2.4 ± 0.4	0.9 ± 0.3	⩾0.999	D
56.0% w/w maltose syrup	27 ± 5	14 ± 4	8 ± 2	21 ± 2	2.2 ± 0.2	1.1 ± 0.4	⩾0.999	D

Post-hoc multiple comparisons using Hotelling tests based on Bonferroni correction $\alpha = 0.05$.
Different letters indicate significant differences at $p \leqslant 0.0001$.
SD: standard deviation.
[a] Controls for the fruit batch used for tests with glucose and trehalose at a_w 0.97.
[b] Controls for the fruit batch used for tests with glucose and trehalose at a_w 0.94.
[c] Control for the fruit batch used for tests with maltose and maltose syrup at a_w 0.97 and 0.94.

Table 5
Mean proton transverse relaxation times and signal percentages of the three components for controls and osmotically dehydrated apples.

Treatment	C_1 (%) ±SD	C_2 (%) ±SD	C_3 (%) ±SD	T_{21} (ms) ±SD	T_{22} (ms) ±SD	T_{23} (ms) ±SD	
Control 0.97 G–T[a]	15 ± 3	18 ± 4	67 ± 2	50 ± 11	205 ± 45	950 ± 60	A
Control 0.94 G–T[b]	17 ± 1	21 ± 2	72 ± 3	57 ± 8	325 ± 20	1207 ± 100	B
Control M–MS[c]	5 ± 1	19 ± 2	76 ± 3	81 ± 10	357 ± 34	1186 ± 61	C
Samples immersed in:							
22.0% w/w glucose solution	24 ± 9	76 ± 9	0	72 ± 25	290 ± 38	0	D
34.4% w/w trehalose solution	40 ± 8	60 ± 9	0	63 ± 12	201 ± 20	0	E
37.3% w/w maltose solution	13 ± 2	40 ± 1	47 ± 2	39 ± 3	114 ± 7	285 ± 16	F
42.0% w/w maltose syrup	18 ± 2	43 ± 3	39 ± 5	44 ± 4	135 ± 15	360 ± 44	G
38.7% w/w glucose solution	27 ± 1	73 ± 1	0	56 ± 5	337 ± 12	0	H
48.0% w/w trehalose solution	39 ± 3	61 ± 3	0	31 ± 4	215 ± 20	0	I
51.0% w/w maltose solution	53 ± 1	47 ± 1	0	38 ± 4	132 ± 4	0	J
56.0% w/w maltose syrup	54 ± 3	46 ± 3	0	39 ± 3	142 ± 13	0	J

Post-hoc multiple comparisons using Hotelling tests based on Bonferroni correction $\alpha = 0.05$.
Different letters indicate significant differences at $p \leqslant 0.0001$.
SD: standard deviation.
[a] Controls for the fruit batch used for tests with glucose and trehalose at a_w 0.97.
[b] Controls for the fruit batch used for tests with glucose and trehalose at 0.94.
[c] Control for the fruit batch used for tests with maltose and maltose syrup at a_w 0.97 and 0.94.

deformation at 100 s) of treated apples were rather similar to those of untreated ones (21% for control 0.97 G–T; 18% for control 0.94 G–T; 17% for control M–MS and for apples immersed in 0.97 a_w maltose, 0.97 a_w maltose syrup and 0.94 a_w maltose solutions; 19% for apple immersed in 0.94 a_w trehalose solution; 16% for apple immersed in 0.96 a_w maltose syrup solution and 24% for apple immersed in 0.97 a_w trehalose solution).

According to Jackman and Stanley (1995b), instantaneous elastic compliance J_0 would be related to the combination of turgor and primary cell wall strength as dictated by cellulose; viscoelastic compliances J_1 and J_2 could be attributed to time – dependent changes in pectins and hemicelluloses respectively, and steady state viscosity could be related to cell wall fluidity arising from exosmosis and/or solubilization and degradation of polymers and less water binding capacity due to treatments. J_0 parameter values (influenced by the same structure elements than G') decreased due to loss of turgor and probably microfibrils reorientation; compliances J_1 and J_2 increased because of folding and loosening of walls and cell wall fluidity increase arised from exosmosis and/or solubilization and degradation of wall macromolecules.

3.4. Water mobility characterization

^{1}H NMR studies indicated different water populations with different distribution and mobility after the osmotic processes. Treated apples showed faster relaxation rates than fresh apple. From CMPG sequence, three populations were detected in fresh apple and in apples dehydrated to a_w 0.97 with maltose and maltose syrup solutions; meanwhile only two populations were noticed in all apples with a_w 0.94 and in apples dehydrated to a_w 0.97 with glucose and trehalose solutions (Table 5). The MANOVA of CPMG parameters indicated significant differences ($F_{50,795} = 39.67$; $p < 0.0001$) in the transverse relaxation response between all samples with the exception of those dehydrated with maltose or maltose solutions with a_w 0.94. The first two discriminant functions explained 93.4% and 3.5% of the variance, respectively. The first contrasted C_1 and C_2 positively and T_{23} negatively and the second axis was defined positively by C_1 and T_{23} and negatively by T_{21} (bi-plot not shown). DFA successfully allowed classifying the 91% of the random apple samples ($n = 170$) by treatments.

In concordance with previous findings of Vicente et al. (2012) using glucose or trehalose as solutes, T_{22} values slightly increased

when the solute concentration increased for both maltose and maltose syrup treated apples. On the contrary, the relative amplitude of signals C_2 and C_1 differed for both a_w assayed: a substantial increase in the least mobile population occurred, suggesting marked changes in water distribution with the increase in maltose or maltose syrup concentration, meanwhile this distribution was not modified in apples treated with glucose or trehalose. T_{21} values remained approximately constant as concentration of maltose or maltose syrup increased, while in the case of glucose and trehalose treatments, T_{21} values decreased with solute level.

Proton relaxation in osmotically dehydrated fruits is obviously a complex phenomenon that depends on several factors and that cannot be easily explained for the different solutes/concentrations studied. In the water-rich region, intrinsic proton relaxation time in a particular sub-cellular compartment is related to the proton chemical exchange between water and biopolymers and/or solutes inside the compartment. But also water molecules are in diffusive exchange between sub-cellular compartments. This last phenomenon can produce an averaging of the intrinsic relaxation times and of the observed relative amplitudes of water present at the different compartments or sites. If there is no exchange between sub-compartments (or if the exchange is slow compared to the experimental NMR time-frame), each site will have its own well defined T_{2i}. On the other hand, if the spins move very fast and freely between the sites, they would lose their site-individuality and only a single averaged parameter will be observed. At an intermediate degree of diffusive exchange, spins of one sub-compartment will partially experience the conditions of the other sub-compartment and the observed relaxation will lose the distinctiveness of the two sites, but still will give some information about interactions between the two systems (Snaar and Van As, 1992; Hills et al., 1990; Hills and Duce, 1990; Vittadini, 2007).

The transverse relaxation of water protons in fresh apple tissues was triexponential and much faster than in bulk water. Integer tonoplast and plasmalemma membranes (see Figs. 1A and 2A) constituted important barriers to water transport and the three decay components would characterize water localized in different sub-cellular components (Raffo et al., 2005; Snaar and Van As, 1992; Hills and Remigereau, 1997; Vicente et al., 2012). The shortest transverse relaxation time T_{21} could distinguish water associated with cell walls, and would be the result of chemical exchange effect due to fast proton exchange between water and hydroxyl protons on the rigid cell wall polysaccharides (pectin, cellulose, hemicellulose). The intermediate relaxation time T_{22} could be attributed to water residing in the cytoplasm and could be explained on the basis of a proton chemical exchange between water and proteins of the cytoskeleton and enzymes and the high viscosity of the cytosol. The highest relaxation time T_{23} could be assigned to water located within the vacuole, arising from the chemical exchange with sugars and other low weight compounds that constitute the dilute solution of the sap. There were significant differences in relaxation parameters among control samples, in some cases greater than 30% (Table 5), probably due to small differences in water content and maturity of the fruit.

When a_w was reduced to 0.97, intrinsic relaxation time values of the protons inside cells would be reduced by increased chemical exchange due to the accumulation of soluble sugars between the wall and the plasmolyzed cytoplasm and the vacuoles and the loss of water from vacuoles (when membranes were not broken) or inside the whole cell (in the case of broken membranes). In addition, these intrinsic relaxation time values would be averaged by water molecular diffusion through field gradients facilitated by increased membranes permeability and/or reduction of the dimensions of vacuoles and cytoplasm. Depending on the interactions of diffusion coefficient, morphology and relaxation rate, data for 0.97 a_w apple fruit showed a double exponential relaxation (glucose and treha-

lose systems) or a triple exponential relaxation (maltose and maltose syrup systems). Protonic sites with T_{23} and/or T_{22} values would be associated with intracellular water while protonic sites with T_{21} values would be associated with extracellular water in the wall.

Unexpectedly and in concordance with previous reports on apple tissues impregnated with glucose or trehalose (Vicente et al., 2012), T_{22} values of maltose and maltose syrup containing apple tissues slightly increased when a_w was reduced to 0.94. The release of water held in hydration layers of membranes, which undergone an important collapse or rupture (Fig. 1F–I), and a consequent reduction in the surface available for swelling after the osmotic treatment, would counteract the greater amount of sugars, the lower moisture content and the smaller volumes for water diffusion of collapsed tissues with a_w 0.94 compared with tissues with a_w 0.97.

Mean values of T_{21} and T_{22} were significantly affected by the nature of sugar(s) used for osmosis: at any a_w T_{2i} values were in the order glucose > trehalose > maltose syrup > maltose treated tissues. The soluble solid content of apple tissues impregnated with the different solutes could partially explain this behavior, but also the type of sugar and the interaction with water must be considered. For instance, a_w 0.94 – maltose syrup treated apples had a lower solid content but a lower interaction with water than a_w 0.94 – maltose apples.

Less mobile water molecules in the wall compartment exhibited relaxation times rather similar to those of fresh apples. It is to be noticed that the small T_{21} values of trehalose (a_w 0.94) and maltose (a_w 0.94 and 0.97) treated tissues are in line with the notorious interaction between these sugars and pectic substances of the cell wall, evidenced in Fig. 2D,G, and H.

Relative amplitude values C_1, C_2 and C_3 of osmosed apples compared with those of fresh fruit would suggest that some water molecules "moved" from the populations inside the cell with intermediate and high mobility to the least mobile population located in the wall, and/or that removed water mainly proceeded from vacuole and cytoplasm. The first possibility would be supported by the greater fluidity ($1/\eta_0$) exhibited in the creep test by treated apples (mainly maltose and maltose syrup treated apples), while cytoplasm contraction (mainly at a_w 0.94) accounted for the second one.

4. Conclusions

Osmotic dehydration induced structural changes in apple tissues, affecting rheological properties. Osmotically dehydrated apples became soft, extensible and lost crispness and hardness. The behavior of the moduli G' and G'' indicated weaker gels after osmosis. There was an abrupt change in compression properties of the tissues after osmotic dehydration at a_w 0.97, while reduction to a_w 0.94 lead to mechanical properties more similar to those of fresh apples. The nature of the sugar employed and the a_w level significantly affected the compression behavior and the state and distribution of water in apple tissues, while in general mechanical spectra and creep analysis were not sensitive enough for distinguishing physical differences between treatments assayed. Some macroscopic rheological parameters could be linked to changes at microscopic level.

Acknowledgements

References

Alzamora, S.M., Cerrutti, P., Guerrero, S., López-Malo, A., 1995. Minimally processed fruits by combined methods. In: Barbosa-Cánovas, G.V., Welti-Chanes, J. (Eds.), Food Preservation by Moisture Control: Fundamentals and Applications. Technomics Publishing Co, Lancaster, USA, pp. 463–492.

Alzamora, S.M., Castro, M.A., Nieto, A.B., Vidales, S.L., Salvatori, D.M., 2000. The rol of tissue microstructure in the textural characteristics of minimally processed fruits. In: Alzamora, S.M., Tapia, M.S., López-Malo, A. (Eds.), Minimally Processed Fruits and Vegetables. Aspen Publishers Inc., Maryland, USA, pp. 153–171.

Alzamora, S.M., Viollaz, P.E., Martínez, V.Y., Nieto, A.B., Salvatori, D.M., 2008. Exploring the linear viscoelastic properties structure relationship in processed fruit tissues. In: Gutiérrez-López, G.E., Barbosa-Cánovas, G.V., Welti-Chanes, J., Parada-Arias, E. (Eds.), Food Engineering: Integrated Approaches. Springer, New York, USA, pp. 133–214.

Calzada, J.F., Peleg, M., 1978. Mechanical interpretation of compressive stress–strain relationships of solid foods. Journal of Food Science 43, 1087–1092.

Carpita, N.C., Gibeaut, D.M., 1993. Structural models of primary cell walls in flowering plants: consistency of molecular structure with the physical properties of the walls during growth. Plant Journal 3, 1–30.

Ceroli, P., 2009. Efecto del soluto durante la deshidratación-impregnación con azúcares en las características mecánicas de tejido de manzana y de melón a altas deformaciones. Thesis Maestría en Bromatología y Tecnología de la Industrialización de Alimentos. Universidad de Buenos Aires, Argentina.

Crowe, L.M., Reid, D.S., Crowe, J.H., 1996. Is trehalose special for preserving dry biomaterials? Biophysical Journal 71, 2087–2093.

Ferrando, M., Spiess, W.E.J., 2001. Cellular response of plant tissue during the osmotic treatment with sucrose, maltose, and trehalose solutions. Journal of Food Engineering 49, 115–127.

Galmarini, M.V., Chirife, J., Zamora, M.C., Perez, A., 2008. Determination and correlation of the water activity of unsaturated, supersaturated and saturated trehalose solutions. Lebensmittel Wissenschaft und Technologie 41, 628–631.

Hills, B.P., Duce, S.L., 1990. The influence of chemical and diffusive exchange on water proton transverse relaxation in plant tissues. Magnetic Resonance Imaging 8, 321–331.

Hills, B.P., Remigereau, B., 1997. NMR studies of changes in subcellular water compartmentation in parenchyma apple tissue during drying and freezing. International Journal of Food Science and Technology 32, 51–61.

Hills, B.P., Takacs, S.F., Belton, P.S., 1990. A new interpretation of proton NMR relaxation time measurements of water in food. Food Chemistry 37, 95–111.

Jackman, R., Stanley, D., 1995a. Perspectives in the textural evaluation of plant foods. Trends in Food Science and Technology 6, 187–194.

Jackman, R.L., Stanley, D.W., 1995b. Creep behaviour of tomato pericarp tissue as influenced by ambient temperature ripening and chilled storage. Journal of Texture Studies 26, 537–552.

Khan, S.A., Roger, J.R., Raghavan, S.R., 1997. Rheology: tools and methods. In: The National Academy of Sciences (Ed.), Aviation Fuels with Improved Fire Safety. Proceedings. Washington DC, USA.

Lewicki, P.P., 2004. Water as the determinant of food engineering properties. A review. Journal of Food Engineering 61, 483–495.

Lillford, P.J., 2001. Mechanisms of fracture in foods. Journal of Texture Studies 32, 397–417.

Mittal, J.P., Mohsenin, N.N., 1987. Rheological characterization of apple cortex. Journal of Texture Studies 18, 65–93.

McGarigal, K., Cushman, S., Stafford, S., 2000. Multivariate Statistics for Wildlife and Ecology Research. Springer-Verlag, New York, USA.

Norrish, R.S., 1966. An equation for the activity coefficients and equilibrium relative humidities of water in confectionery syrups. Journal of Food Technology 1, 25–39.

Patist, A., Zoerb, H., 2005. Preservation mechanisms of trehalose in food and biosystems. Colloids and Surfaces B: Biointerfaces 40, 107–113.

Peleg, M., 1984. A note on the various strain measurements at large compressive deformations. Journal of Texture Studies 15 (4), 317–326.

Pitt, R., 1992. Viscoelastic properties of fruits and vegetables. In: Rao, M.A., Steffe, J.F. (Eds.), Viscoelastic Properties of Foods. Elsevier, London & New York, pp. 49–76.

Pizzocaro, F., Torreggiani, D., Gilardi, G., 1993. Inhibiton of apple polyphenoloxidase (PPO) by ascorbic acid, citric acid and sodium chloride. Journal of Food Processing and Preservation 17, 21–30.

Quinn, G.P., Keough, M.J., 2002. Experimental design and data analysis for biologists. Cambridge University Press, New York, USA.

Raffo, A., Gianferri, R., Barbieri, R., Brosio, E., 2005. Ripening of banana fruit monitored by wáter relaxation and diffusion ^{1}H NMR measurements. Food Chemistry 89, 149–158.

Resnik, S.L., Favetto, G., Chirife, J., Ferro Fontán, C., 1984. A world survey of water activity values of certain saturated solutions at 25 °C. Journal of Food Science 49, 510–516.

Reynolds, E.S., 1963. The use of lead citrate at high pH as an electron opaque stain in electron microscopy. Journal of Cell Biology 17, 208–212.

Sherman, P., 1970. Industrial Rheology. Academic Press, New York, USA.

Snaar, J.E.M., Van As, H., 1992. Probing water compartments and membrane permeability in plant cells by ^{1}H NMR relaxation measurements. Biophysical Journal 63, 1654–1658.

Sorrivas, V., Morales, A., 1983. Introducción a la Microscopía Electrónica . Centro Regional de Investigaciones Básicas y Aplicadas de Bahía Blanca & Banco del Sud, Bahía Blanca, Argentina.

Vicente, S., Nieto, A.B., Hodara, K., Castro, M.A., Alzamora, S.M., 2012. Structure, rheology, and water mobility of apple tissue induced by osmotic dehydration with glucose or trehalose. Food and Bioprocess Technology 5, 3075–3089.

Vittadini, E., 2007. Effects of water distribution and transport on food microstructure. In: McClements, J. (Ed.), Understanding and Controlling the Microstructure of Complex Foods. Woodhead Publishing Limited, Cambridge, England, pp. 89–112.

Waldron, K.W., Smith, A.C., Parr, A.J., Ng, A., Parker, M.L., 1997. New approaches to understanding and controlling cell separation in relation to fruit and vegetable texture. Trends in Food Science and Technology 8, 213–221.

Waldron, K.W., Parker, M.L., Smith, A.C., 2003. Plant cell walls and food quality. Comprehensive Reviews in Food Science and Food Safety 2, 128–146.

Wilson, R.H., Smith, A.C., Kacuracova, M., Saunders, P.K., Wellner, N., Waldron, K.W., 2000. The mechanical properties and molecular dynamics of plant cell wall polysaccharides studied by Fourier-transform infrared spectroscopy. Plant Physiology 124, 397–405.